Oxygen-vacancy phase equilibria in $YBa_2Cu_3O_z$ calculated by the cluster variation method

A. Berera
Department of Physics, University of California, Berkeley, California 94720

D. de Fontaine
Department of Materials Science and Mineral Engineering, and Materials and Chemical Sciences Division, Lawrence Berkeley Laboratory, University of California, Berkeley, California 94720

(Received 31 May 1988)

Ordering in the Cu-O basal plane of $YBa_2Cu_3O_x$ is investigated as a function of oxygen content, chemical potential, and temperature. Two phase diagrams are calculated by means of the cluster variation method applied to asymmetric two-dimensional Ising models with one nearest-neighbor and two second-nearest-neighbor interactions. The interaction parameters selected ensure the stability of the orthorhombic structures near $z=7$ and for one of the cases also includes a cell-doubling phase at $z=6.5$. Oxygen pair and point probabilities are studied as a function of temperature under conditions of constant oxygen partial pressure. Comparison of site occupancy and orthorhombic-to-tetragonal second-order transition temperatures with recent experimental data are in excellent agreement.

I. INTRODUCTION

It is now recognized that, in the three classes of high-T_c oxides recently discovered, the La compounds,[1] the $YBa_2Cu_3O_z$ (1:2:3) compound[2] (and those related to it by various cation substitutions), and the Bi-containing compounds,[3] superconductivity originates in CuO_2 planes. The remainder of the structure appears to play a secondary but decisive role, that of providing the right electronic environment for the copper oxide planes. In the 1:2:3 compound, oxygen holes in CuO_2 sheets (rumpled planes), and in Cu-O chains along the b direction both appear to be responsible for conductivity.[4] Plane-to-chain coupling may be required for superconductivity, but clearly, in the absence of chains, the material is not a superconductor.[5] A thorough understanding of the thermodynamics of chain formation is thus crucial to the preparation and optimization of properties of the 1:2:3 compound.

Early on, it was recognized that chain formation, which is accompanied by a tetragonal-to-orthorhombic transition, can be regarded as resulting from an oxygen ordering instability in the Cu-O plane containing the chains.[6] This plane (not the rumpled CuO_2 plane) will be called here "the basal plane," for want of a better designation. In a purely formal way, the ordering transition could be represented by means of a two-dimensional Ising model featuring isotropic nearest-neighbor and anisotropic next-nearest-neighbor effective pair interactions. This model, to be briefly reviewed in the next section, predicted possible cell-doubling and cell-quadrupling structures[6,7] and led to the calculation of order-disorder phase diagrams[8-11] based on empirically chosen effective pair interaction (EPI) parameters. The statistical method used was the cluster variation method (CVM), briefly described in Sec. III. New calculated phase diagrams will be presented in Sec. IV, and the calculation of oxygen partial pressure curves will be described in Sec. V. Oxygen pair correlations will be presented in Sec. VI and the results discussed in Sec. VII.

II. EFFECTIVE PAIR INTERACTIONS

The planar model adopted is that shown in Fig. 1. The basal plane structure can be regarded as made up of three interpenetrating square sublattices; one of Cu atoms, two of oxygen sites, the latter two being labeled α and β. In the tetragonal phase, O and □ symbols occupy oxygen sites statistically so that the planar symmetry is $p4mm$. In the orthorhombic superconducting phase, the basal (chain containing) plane's structure has rectangular symmetry ($p2mm$), and sublattice α is primarily occupied by O and β by □ symbols, or vice versa. The former structure is de-

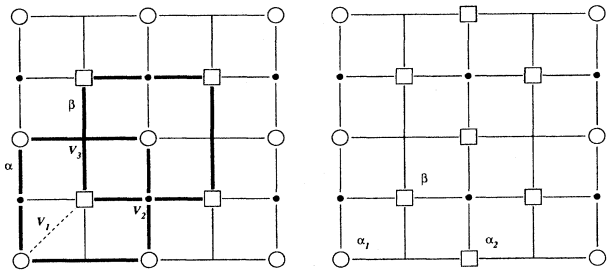

FIG. 1. Cu_2O basal plane model. (a): Ground-state configuration at $c_0=0.5$. Small filled circles denote Cu atoms, O denotes oxygen, and □ denotes vacant sites. Two sublattices α and β are present. Pair interactions V_1, V_2, V_3 are indicated. (b): Ground-state configuration at $c_0=0.25$. Three sublattices α_1, α_2, and β form in the cell-doubling phase.

picted in Fig. 1(a). As explained below, other two-dimensional ordered structures are possible, in particular, a double-cell structure in which the α sublattice splits into two nonequivalent ones, labeled α_1 and α_2 in Fig. 1(b). This structure, to be discussed further, will be called "ortho II" ($p2mm$II) to distinguish it from the (single-cell) "chain" structure, henceforth designated as ortho I. The Cu sublattice has fixed occupancy and plays no role in the oxygen ordering process; the Cu atoms do break the symmetry of the oxygen site array, however, in a very essential way.

The smallest set of interaction parameters capable of providing the appropriate physics to the problem is now introduced: one nearest-neighbor V_1, and two next-nearest-neighbor interactions, V_2 and V_3, the first mediated by a Cu atom, the second not. The EPI's V_n, can be given a rigorous definition derived directly from the cluster variation method (CVM) formulation:[12,13]

$$V_n = \tfrac{1}{4}[V_n(\mathrm{O},\mathrm{O}) + V_n(\square,\square) - 2V_n(\mathrm{O},\square)], \quad (n=1,2,3), \tag{1}$$

where $V_n(I,J)$ [I,J=O, oxygen; □, vacant site] represents the energy of the system containing the specified I,J pair, in nth neighbor position, embedded in a medium whose sites are occupied randomly by O or □ with specific oxygen concentration c_0. Generally, EPI's are thus expected to be concentration dependent.[14,15] Here, for simplicity, the V_n will be taken as concentration independent.

The EPI's should not be confused with "pair potentials," and the total energy of a crystalline solid in no way consists of a sum of EPI's. Indeed, the V_n represent only ordering energies, and their magnitude is very small compared to the cohesive energy of the material. From theoretical considerations[14,15] and direct computations,[13] it was shown that the V_n even in good metals, particularly transition elements and alloys, form a rapidly convergent set. Apparently, the long-range portion of the pair potentials tends to cancel by taking differences in Eq. (1), leaving only short-range effective interactions.

In the orthorhombic phase, Cu ions are fourfold coordinated to oxygens in both rumpled plane and chain environments. In the latter, the coordinated oxygen sites are the two adjacent 01 (along the b axis, that of the chain) and the two 04 sites (along the z axis, out of the basal plane). Given that bonding orbitals are the Cu $d_{z^2-y^2}$ and the O p_y, it follows that O—O bonds bridged by Cu will be highly favorable whereas nearest-neighbor O—O bonds *in* the basal plane, which would tend to produce sixfold coordination, are highly unfavorable. In terms of effective pair interactions, these arguments, according to Eq. (1), predict large positive (repulsive) V_1 and large negative (attractive) V_2 interactions. The sign of V_3 cannot be determined by such considerations, but the magnitude of this unmediated second-neighbor interaction is probably small compared to that of V_1 and V_2.

The important parameters which determine ordering in the basal plane are thus the ratios $x=V_2/V_1$ and $y=V_3/V_1$. All possible ordering arrangements of O and □ on oxygen sites were determined[7] for all possible values of x and y, with $V_1>0$. In addition to the disordered arrangement, which corresponds in three dimensions to the tetragonal phase, seven two-dimensional ordered ground states were found, four at stoichiometry $c_0=0.50$, three at stoichiometry $c_0=0.25$ (or 0.75). Ordering maps were derived which show regions in the x,y plane where a particular structure has lowest energy.[7,9,11] As expected from the qualitative discussion of EPI's just given, the chain structure (orthorhombic phase) is stabilized by $V_2<0$ at $c_0=0.50$. For V_3, also negative, two-phase coexistence of tetragonal and orthorhombic structures is predicted for any concentration in the interval $0<c_0<\frac{1}{2}$, corresponding to the interval $6<z<7$, where z is the stoichiometry index in $YBa_2Cu_3O_z$. For $V_2<0$, $0<V_3<1$ a double-cell orthorhombic structure is predicted at stoichiometry $c_0=0.25$, i.e., $z=6.5$. This structure, denoted ortho II [Fig. 1(b)] is the one found experimentally by transmission electron microscopy.[16,17] Ortho II differs from ortho I in that chains along the b direction are alternately occupied and unoccupied by O atoms. Ortho II appears to be a distinct ordered phase with a superconducting transition temperature of about 60 K.[18]

III. STATISTICAL MODEL

If second-neighbor interactions are included, the two-dimensional Ising model can no longer be solved analytically. Previously, Monte Carlo simulation[19] and renormalization-group theory[20,21] have been used to calculate phase diagrams for the symmetric case $V_2=V_3$. For the asymmetric case $V_2\neq V_3$, we used the CVM, first suggested by Kikuchi,[22] as an analytical approximation to the Ising problem. The application of the CVM to the calculation of phase diagrams was initially carried out by van Baal,[23] and recently reviewed by one of the present authors[24] in the formulation proposed by Sanchez, Ducastelle, and Gratias.[25]

The basic idea of the CVM is to replace the sum over states in the partition function by its maximum term and then to enumerate only the number of configurations that can be generated by a small set of basic clusters. Recently,[26] rules have been proposed for the selection of suitable clusters for a given problem. At the very least, the basic clusters must contain the effective interactions required in the energy formulation. Here, following earlier work,[26,27] the 4-point/5-point combination was chosen, consisting of a rhombohedron and a centered rectangle.[8] The free energy can then be expressed as a functional in a set of multisite correlation functions ξ_j, the index j labeling correlations pertaining to the basic clusters chosen and all of their subclusters.

Table I (Ref. 24) lists the basic 5-point (No. 11) and 4-point (No. 8) clusters and their subclusters down to the point cluster (No. 0), as required for the ortho-I phase. For this phase, 25 clusters are required. For the disordered phase, the α and β varieties are no longer distinct, neither are Nos. 2 and 3 and Nos. 5 and 5′; hence, only 11 clusters are required. For ortho II, the α sublattice further splits into α_1 and α_2 [Fig. 1(b)]; hence, 41 distinct clusters result.

The CVM free energy functional, per O site, for the

TABLE I. Clusters required for CVM description of ortho-I phase (Ref. 24).

i	α	β	i	α	β
0					
1			6		
2			7		
3			8		
4			9		
5			10		
5′			11		

present case is

$$F=\sum_{i=1,2,3} n_i V_i \xi_i + k_B T \sum_j \gamma_j \sum_\sigma x_j(\sigma) \ln x_j(\sigma) , \quad (2)$$

where k_BT are Boltzmann's constant and the absolute temperature, respectively, n_i are the number of pairs ($i=1,2,3$) per site, $x_j(\sigma)$ are cluster concentrations for each possible configuration $\{\sigma\}$ of O and □ on cluster sites, and the integers γ_j are so-called Kikuchi-Barker coefficients which may be determined by appropriate recursion formulas.[24,25] For clusters indicated in Table I, for the disordered phase, one finds $\gamma_1=2$, $\gamma_5=\gamma_{5'}=4$, $\gamma_8=-1$, and $\gamma_{11}=-1$, with the other coefficients being zero. Cluster concentrations x_j can be expressed as linear functions of the correlations ξ_i, the latter being the independent variables of the problem.[28] The V_i are the three EPI's previously defined.

In the spirit of the variational procedure, the functional F must then be minimized with respect to the ξ variables. Thus, the method returns not only an approximate (minimized) free energy for each phase considered, as a function of T and of the average concentration $c_0=x_0(\mathrm{O})$, but also the equilibrium values of multisite correlations or, equivalently, cluster concentrations x. Hence, the CVM can describe short-range as well as long-range order.

IV. PHASE DIAGRAM

Some CVM phase-diagram calculations pertaining to the 1:2:3 compound's basal plane have been presented elsewhere.[8-11] Here, two new calculations are reported. Calculations performed by others have been limited to the symmetric case ($V_2=V_3$) only, in the CVM square approximation[29] (cluster No. 8 in Table I), in the pair (quasichemical) approximation (clusters No. 1 and No. 2),[30] and in the "point" approximation (cluster No. 0, Bragg-Williams approximation).[31,32] Recently, a Monte Carlo simulation has been performed with $V_2 \neq V_3$.[33] Generally, the accuracy of the approximation improves with the size of the largest cluster(s). In the case of a two-dimensional Ising model with nearest-neighbor coupling V_1, the exact transition temperature (at $c_0=0.5$) obtained by Onsager is $2.268V_1$, whereas the "point" Bragg-Williams approximation gives a critical temperature of $4.0V_1$ and the pair gives $2.885V_1$. The 4-point/5-point CVM approximation used in the present calculations overshoots the true critical temperature by 4%, giving $2.359V_1$.[26,34]

To test the method, the following parameters were initially chosen: $V_1>0$, $V_2=V_3=-0.5V_1$, since renormalization-group[20,21] and Monte Carlo[19] calculations were available for comparison. As described elsewhere,[8] the CVM-calculated phase diagram featured a second-order transition line between tetragonal and ortho-I phases at high temperatures, terminating at low temperature by a tricritical point below which phase separation occurs between these two structures, the general topology being that of the diagram shown in Fig. 2. With concentration-independent pair interactions, the phase diagram is symmetric about the midconcentration $c_0=0.5$; hence, only the left portion of the diagram is shown. The CVM, being a mean-field (albeit improved) theory, tends to overestimate critical temperatures, and gives phase

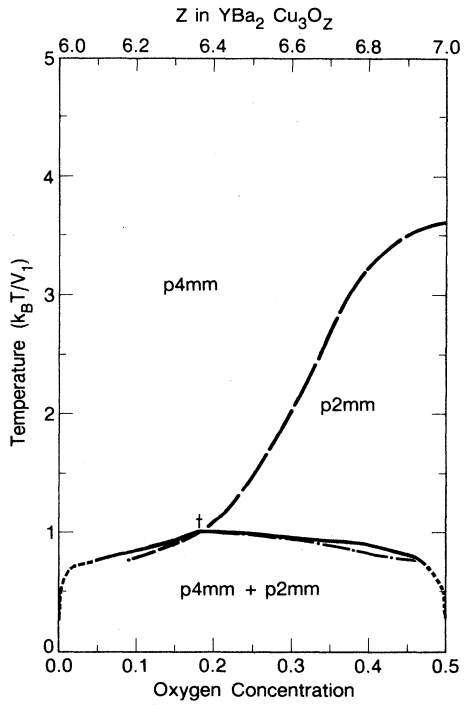

FIG. 2. CVM phase diagram calculated for $V_1=1$, $V_2=-0.50$, $V_3=-0.25$. Second-order transitions indicated by dashed lines, miscibility gap by full lines. Thin dashed line is metastable extension of the second-order line, then dot-dashed curve is the line of marginal instability for phase separation on the partially filled oxygen sublattice. Tricritical point is at point marked t. Orthorhombic and tetragonal phase regions are labeled as *p4mm* and *p2mm*, respectively, and two-phase region as *p4mm*+*p2mm*. Upper axis relates planar concentration (c_0) to overall oxygen stoichiometry $z=2c_0+6$.

boundaries that are too "pointed" at the tricritical point; a more exact calculation shows a flatter miscibility gap. Nevertheless, improvement over Bragg-Williams approximations is considerable.

A. Tricritical model

Figure 2 shows the qualitatively similar case of $V_1 > 0$, $V_2/V_1 = -0.50$, $V_3/V_1 = -0.25$, which, according to ground-state analysis, should produce only the tetragonal (tetra) and ortho-I phases. It should be noted that rules derived by Allen and Cahn[35] on the basis of Landau theory relative to extrapolated transition lines and spinodals are well obeyed by the CVM results: The O-poor phase boundary is tangent at the tricritical point (t) to the line of second-order transitions, itself extended into the two-phase coexistence region in an ordering spinodal[36] (fine dashed lines). The fine dot-dashed curve represents the "conditional spinodal."[35]

Salient features of the CVM diagrams are summarized in Table II. It is seen that, for diagrams 1 and 2, the latter has a lower critical temperature, T_c at $c_0 = 0.5$ by $0.41\tau_t$ (where τ is the reduced temperature $k_B T/V_1$), reflecting its decreased ability to sustain order. The tricritical point in 2 occurs at $\tau_t = 1.02$, $c_0 = 0.185$, and $\mu = -3.957$ (in units of V_1). It is lower by 0.39τ in temperature and 0.005 in concentration compared to 1. The gap between T_t and T_c diminishes by 0.12τ in 2 and is at 28.2% of critical temperature, compared to 35% in 1. For both diagrams the numerical algorithm used in the calculations converges with difficulty at low temperatures, hence, the lower portion of the miscibility gap, below $0.8\tau_b$ of Fig. 2, was not computed precisely, but constructed in accordance with Monte Carlo results.

B. Cell-doubling model

There is now ample evidence for the existence of another ordered phase in the 1:2:3 system[17,18,37] that of the ortho-II structure mentioned above. Ground-state analysis[7] shows clearly that, as soon as V_3 becomes positive, the low-temperature two-phase coexistence region is interrupted by the ortho-II single-phase field. Its domain of existence, with respect to oxygen content, will tend to widen (at nonzero temperature) as V_3 increases. At $T = 0$ K, ortho II should be stable at stoichiometry $c_0 = 0.25$ ($z = 6.5$) only.

Previous CVM calculations performed with $V_2/V_1 = -0.5$, $V_3/V_1 = +0.5$ were reported elsewhere.[10] Figure 3 shows the phase diagram resulting from a new calculation performed with same V_3/V_1 ($= +0.5$) but with $V_2/V_1 = -0.75$. The two diagrams are quite similar, but the bicritical point of the previous calculation has now become a critical end point. Coordinates of the relevant critical (or multicritical) points for these diagrams are also indicated in Table I.

In Fig. 3, only features calculated rigorously by the CVM have been plotted. Low-temperature equilibrium lines should be qualitatively similar to those reported earlier.[10] All diagrams show a line of second-order transitions between *p4mm* (tetragonal phase) and *p2mmI* (ortho I). Differences arise below the multicritical point which terminates the second-order line, and the nature of the multicritical point changes as well. For $0 < V_3 < 1$, the transition between ortho I and ortho II should be second-order on the oxygen-rich side of a tricritical point (not marked) which must exist near the top of the ortho-II phase region. At lower temperatures, the ortho-I/ortho-II line of second-order transitions should terminate at another tricritical point, below which a wide ortho-I and ortho-II coexistence region should be found, with each ordered phase stable at its respective stoichiometry only. The general appearance, at low temperature, should be that of the cell-doubling phase diagram published previously.[10]

Details of the top portion of the ortho-II phase region are shown in Fig. 4. On the oxygen-poor side of the upper-tricritical point, the transition is first order. The two-phase region is between ortho I and II for a small interval from $\tau = 1.30$ to $\tau = 1.29$ and then between ortho II and tetra for lower temperature. At $\tau = 1.29$, $c = 0.253$, the ortho-I/tetra second-order line (long dashed) intersects the leftmost first-order line (solid) at the critical end point b. The first-order line has a discontinuous slope at the critical end point, with the lower-temperature curve being steeper, as required by the rules derived by Allen and Cahn.[35]

In addition to the two first-order and two second-order phase boundaries which join at the upper portion of the ortho-II phase, also shown in Fig. 4 is the metastable continuation of the ortho-I/tetra second-order line (fine long dashes), and the instability lines of the disordered (chain-dotted) and single-phase orthorhombic (small dashed) phases. All three lines intersect at point p, with the disordered instability tangent and the ortho-I instability veer-

TABLE II. Summary of parameters used in CVM phase diagram calculations and critical temperatures (in units of kT/V_1): T_c denotes second-order critical temperature at $c_0 = \frac{1}{2}$, T_m denotes multicritical temperatures as indicated: T_t, tricritical; T_b, bicritical; T_e, critical end point.

Diagrams	$V_1 > 0$ V_2/V_1	V_3/V_1	T_c (kT/V_1)	T_m (multisite)	Ratios T_m/T_c
1	−0.50	−0.50	4.01	$T_t = 1.41$	0.350
2	−0.50	−0.25	3.62	$T_t = 1.02$	0.282
3	−0.50	+0.50	2.27	$T_b = 0.99$	0.436
4	−0.75	+0.50	2.65	$T_e = 1.29$	0.487

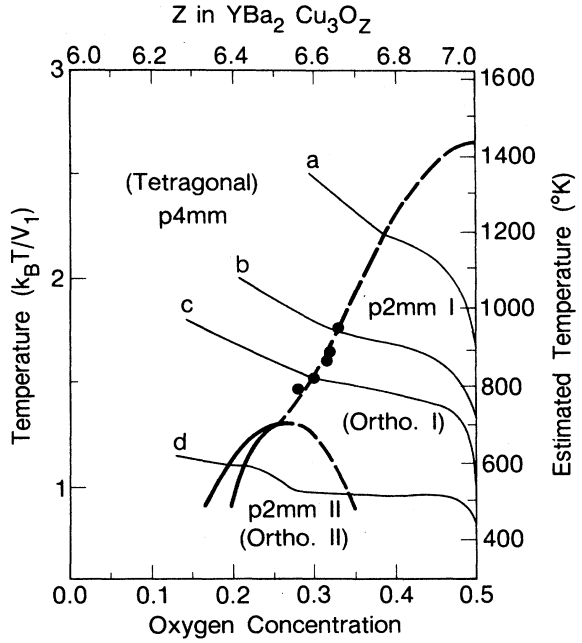

FIG. 3. Cell-doubling phase diagram calculated for $V_1=1$, $V_2=-0.75$, $V_3=0.50$. Second-order transitions indicated by dashed lines, first-order phase boundaries are full lines. Filled circles are experimentally determined (Ref. 38) order-disorder transition points. Fine solid curves *a* through *d* are lines of constant oxygen partial pressure at 400 atm, 1 atm, 0.02 atm, and 10^{-8} atm, respectively.

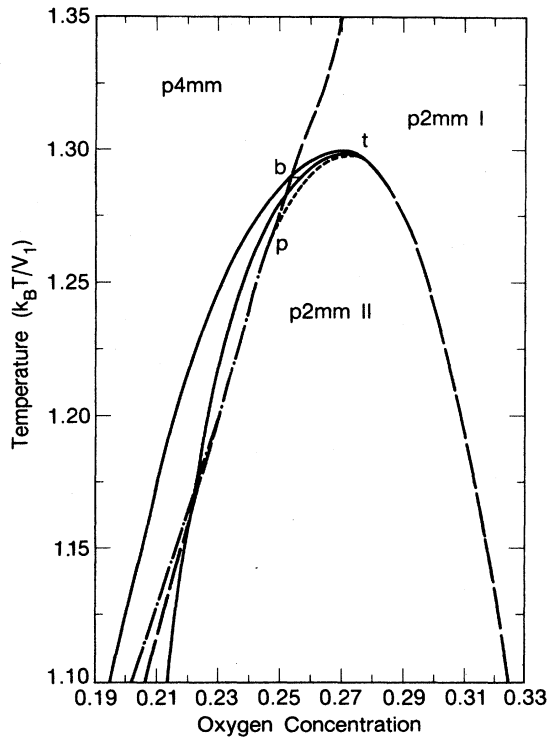

FIG. 4. Enlargement of top portion of ortho-II phase from Fig. 3. Second-order ortho-I/II phase boundary (long-dashed line) bifurcates at the tricritical point *t* into two first-order phase boundaries (solid lines). Ortho-I/tetra second-order line (long-dashed line at top part of figure) crosses the first-order phase boundary at a critical end point *b*. The metastable continuation of the ortho-I/tetra second-order line (long-dashed line at bottom left) starts at *b*, goes through *p*, and continues in direction of decreasing c_0. Ortho-I instability line (small-dashed) and disordered instability line (dot-dashed) meet at *p*.

ing off sharply with respect to the metastable line. For the ortho-I phase, its region of instability is perimetered by the I to II second-order line, the metastable continuation line, and this small-dashed segment. To obtain these boundaries, clusters required for ortho I (Table I) are used in the free-energy functional. Inside the unstable region, the computed extremum is the saddle point since there are "hidden variables" which have been ignored. The domain of the free energy function for ortho I is a 25-dimensional subspace inside the 41-dimensional space defined by the ortho-II free energy function. By restricting to the smaller subspace and over the defined interval of the ortho-I cluster variables, no minimas exist, only saddle points, in the region of ortho-I instability. However, if the additional degrees of freedom given by the set of cell-doubling clusters are introduced, a true minimum is found.

Filled circles in Fig. 3 represent data points, as observed by Specht *et al.*,[38] for the ortho-I to tetra phase transition, for oxygen partial pressures 1.0, 0.2, 0.1, 0.02, and 0.005 atm, in descending order. As was done for the previous cell-doubling phase diagram,[10] the data point for $p_{O_2}=0.02$ was placed on the order-disorder curve at the measured oxygen concentration. This procedure fixed the temperature scale (estimated temperatures are indicated on the right-hand scale of Fig. 3), i.e., fixed the value of the nearest-neighbor EPI which, in the present case, gave the value $V_1\cong 0.048$ eV. It follows that the second-neighbor EPI's must have values $V_2=-0.036$ eV and $V_3=+0.024$ eV. The remaining four experimental points were then found to fall very near the calculated curve with no further fitting. Considerable controversy still exists about the actual values of the oxygen content at the transition, however. This point will be discussed further in Sec. VII. The fine solid lines are calculated curves of oxygen partial pressure: (a) 400 atm, (b) 1 atm, (c) 0.02 atm, (d) 10^{-8} atm. Details of the calculation are given in the next section.

V. OXYGEN PARTIAL PRESSURE

The reaction which consists of exchanging or removing an oxygen atom from the basal plane, replacing it by a vacancy, placing the oxygen atom in the gas phase, and having it react there to form an oxygen molecule can be written symbolically as

$$O=\square+\tfrac{1}{2}O_2, \tag{3}$$

with standard free-energy change per oxygen atom given by

$$\Delta g^0=\tfrac{1}{2}\mu^0_{O_2}-(\mu^0_O-\mu^0_\square) \tag{4}$$

and corresponding enthalpy (Δh^0) and entropy (Δs^0) changes. The equilibrium condition for reaction (3) can be written in terms of chemical potentials as

$$\mu_O = \mu_\square + \tfrac{1}{2}\mu_{O_2}, \tag{5}$$

the subscripts in Eqs. (3) and (4) indicating an oxygen on a crystal site (O), a vacant site (□), and molecular oxygen in the gas phase (O_2); the superscripts (^{0}) denote 1 atm standard states.

The chemical potential μ calculated by the CVM is the difference $(\mu_O - \mu_\square)$, so that, with

$$\mu_{O_2} = g^0_{O_2} + k_B T \ln p_{O_2},$$

we have

$$\mu = \Delta h^0 + T(k_B \ln p_{O_2}^{1/2} - \Delta s^0). \tag{6}$$

The quantity μ on the left-hand side of Eq. (6) is obtained by taking the derivative of the free energy F of Eq. (2) with respect to c_0, the concentration dependence entering through the point correlation function ξ_0.

In Eq. (6), it is understood that the symbol p_{O_2} really stands for a ratio of pressures, with reference pressure taken as 1 atm. If the standard enthalpy and entropy changes are regarded as approximately temperature independent, then Eq. (6) represents a straight line in a (T,μ) coordinate system: The enthalpy change is the intercept of that line at $T=0$ K on the μ axis and the slope varies linearly with the logarithm of p_{O_2}. It then suffices to take two data points from the data[38] used to plot experimental points on the diagram of Fig. 3 to determine the values of Δh^0 and Δs^0. The values obtained by using the Oak Ridge data for $p_{O_2}=1$ atm and 0.02 atm are, approximately, $\Delta h^0 = 0.6$ eV and $\Delta s^0 = 10^{-2}$ eV/K per O site. Two other curves have been calculated with the same Δh^0 and Δs^0 parameters, those labeled (a) for 400 atm and (d) for 10^{-3} atm. For the latter, the reactions are so sluggish at these low temperatures that equilibrium will probably not be attained.

It is instructive to plot the phase diagram and the p_{O_2} curves on a (T,μ) plot, as done in Fig. 5 where both O-poor and O-rich portions are shown. The four isobars of Fig. 3 are now straight lines which all intersect the μ axis at the value $\Delta h^0 = 12.6$ (in units of V_1). At second-order transition points, the p_{O_2} curves change slope on the (T,c_0) diagram; at first-order transitions, the p_{O_2} curves become horizontal straight line segments inside the coexistence regions. The construction of Fig. 5 and resulting p_{O_2} curves of Fig. 3 clearly show that it is quite possible, in principle, to obtain oxygen contents greater than $c_0 = 0.5$ ($z=7$). However, the presence of very wide miscibility gaps at low temperatures forces the p_{O_2} curves to plunge sharply down in the vicinity of $c_0 = 0.5$. Hence, in order to prepare high-oxygen content samples of $YBa_2Cu_3O_x$ at constant oxygen partial pressure, it must be necessary to use high-O_2 overpressures and to anneal a long time at rather low temperatures.

As was done by previous authors,[30] it is possible to use the expression

$$\varepsilon = \Delta h^0 - \tfrac{1}{2}E_d,$$

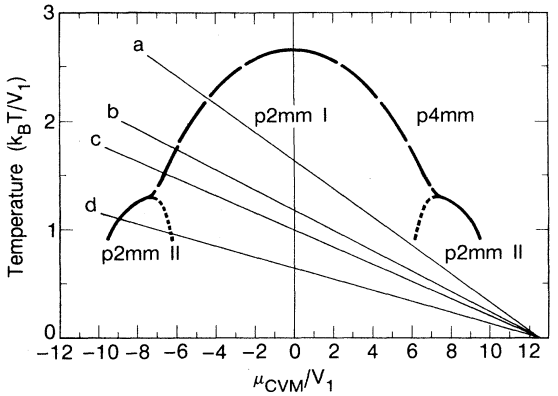

FIG. 5. Both sides of the temperature vs chemical potential phase diagram corresponding to the cell-doubling case of Fig. 3. Long-dashed curve marks the ortho-I/tetra second-order transitions. Small-dashed curve marks the ortho-I/II transitions. First-order lines on the (T,μ) plot join into a single line, shown as the dark solid curves.

to calculate the oxygen site energy ε on the basal plane, E_d being the $O_2 \rightarrow 2O$ dissociation energy. If the latter value is taken to be 5 eV, Δh^0 being taken from the intercept in Fig. 5, the site energy comes out to -3.1 eV, in reasonably good agreement with previously determined values.[10]

VI. OXYGEN SITE AND PAIR CONCENTRATIONS

In Fig. 6 the solid curve shows the calculated fractional site occupancy of O atoms on the α and β sublattices calculated along the 1 atm partial pressure curve (b). The plotted symbols are from experimental measurements taken at 1 atm oxygen partial pressure by Jorgensen *et al.*,[5] with empty (filled) circles from the O-rich (poor) sublattice in the ordered phase and filled squares from the disordered phase.

We kept the same temperature scale as fit to the Oak Ridge data rather than optimize to these new values. Due to the fact that the Argonne transition temperature was 30 K higher than the Oak Ridge value, our curves are shifted with respect to the former data. Nevertheless, the correspondence is still qualitatively fairly good. Note, in particular, for both experimental and theoretical results, the rapid filling of the O-rich (α) sublattice just below the transition temperature and the even more pronounced depletion of the O-poor (β) sublattice. Also consistent with Jorgensen's results is the downward slope of the occupancy line in the disordered phase. For lower temperatures, this agreement breaks down, especially on the α sublattice. Whereas our calculated values tend to 1.0, the experimental curves flatten out near 0.9. This latter effect was surmised by Jorgensen *et al.* to be due to diffusion-limited kinetic effects.[5]

Shown in Fig. 7 along the same 1-atm isobar is the probability of finding an O-O pair in the Cu direction on the α sublattice (cluster on the α sublattice in Table I). The close resemblance of the point and pair probability

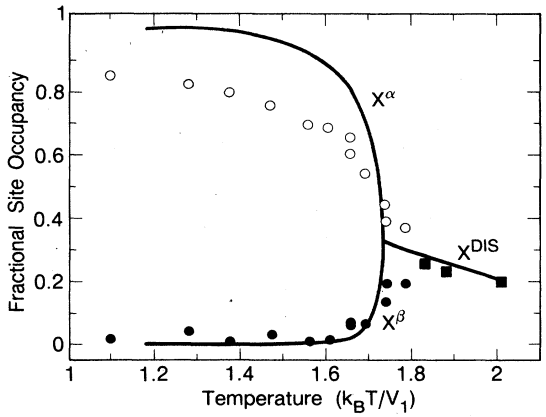

FIG. 6. Fractional site occupancy of O atoms at 1 atm constant oxygen partial pressure. The solid curve gives the calculated results for the oxygen-rich (α) and oxygen-poor (β) sublattices when in the ordered ortho-I phase. The tail beginning at $\tau=1.735$ and extending down with increasing temperature is for the disordered phase. The circular and square symbols are experimental points obtained by Jorgensen *et al.* (Ref. 5).

curves in Fig. 6 and 7, respectively, indicates strong short-range correlation; finding one O atom implies a high probability of finding another O atom next to it. As a quantitative measure of this effect, define the enhancement factor ε as

$$\varepsilon=\frac{x_2^\alpha}{(x_0^\alpha)(x_0^\alpha)},$$

where x_0^α is the point probability on the α sublattice and x_2^α is the pair probability on the α sublattice, in the Cu direction. Quite explicitly, ε is the ratio of the actual pair probability over that expected for random O distribution. ε is approximately 2 at the transition point $\tau=1.735$, larger at higher temperatures, and tends to one for lower temperatures. A large enhancement factor when site occupancy is low, as it is near the transition point, implies clustering tendency among the O atoms. An ε greater than 2 in the tetragonal phase also means that local ordering of O atoms prevails long before long-range order sets in. For decreasing temperature below 1.735, since the oxygen site occupancy approaches unity, this presence of more O atoms forces the random pair probability also to unity, irrespective of short-range correlation effects, hence ε too must approach one.

The pair (along Cu direction as above) and point probabilities were also examined in the cell-doubled region. In this phase, recall that the α sublattice further divides into an oxygen-preferred α_1 sublattice and oxygen-deficient α_2 sublattice. Of most interest is examining the individual behavior of the probabilities and their combined average on these two sublattices. In Fig. 8 the point (solid lines)and pair (dashed lines) probabilities are shown corresponding to the lowest partial-pressure curves. Both were plotted on the same graph to illustrate how strongly the short-range order, due to pairing, is correlated to the long-range order due to site occupancy. The labels α_1 and α_2 are the separate probabilities on these two sublattices, respectively, and α_{av} is the average.

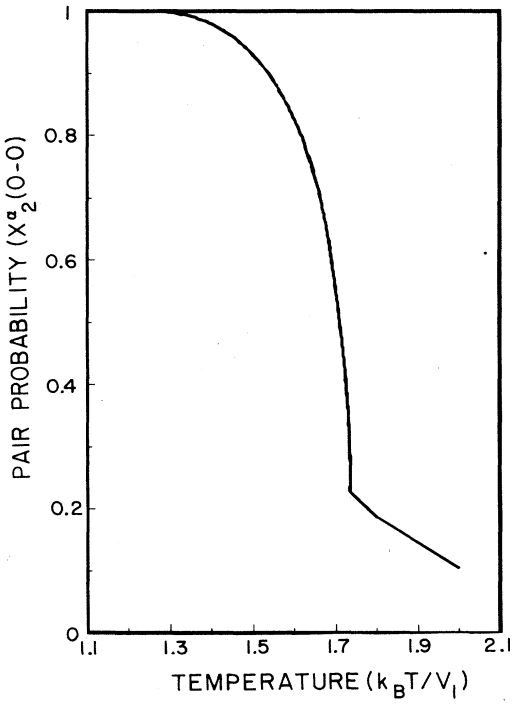

FIG. 7. Oxygen pair probability on the α sublattice in the copper-mediated direction at 1 atm oxygen partial pressure (along isobar *b* in Fig. 3).

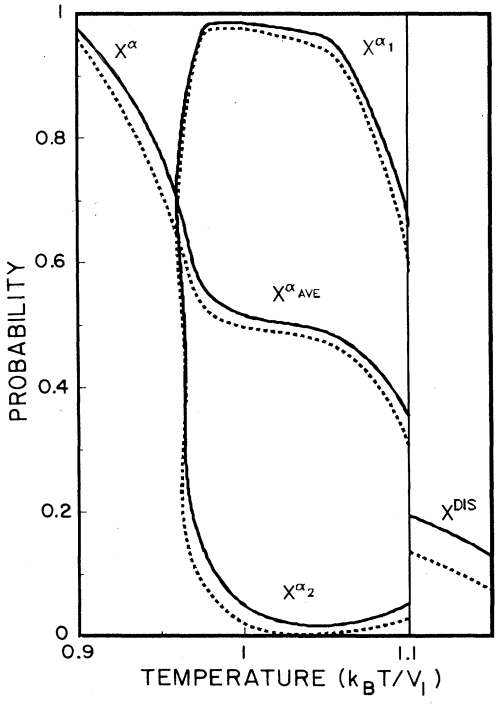

FIG. 8. Point probabilities (solid curves) and pair probabilities in copper-mediated direction (dashed curves) along isobar *d* in Fig. 3. Vertical line at $\tau=1.10$ indicates the first-order transition between tetra and ortho-II phases.

The point probability in the disordered phase behaves similarly to that in Fig. 6. At the temperature $\tau=1.1$, there is a discontinuous shift which is characteristic of the first-order transition. From here down to $\tau=0.96$, the cell-coupling region stabilizes, thus producing three separate point probabilities associated with the three sublattices. On the α_1 sublattice the influx of O atoms increases dramatically just as ordering occurs. The occupancy is close to 100% in the entire cell-doubled region. It then makes a sharp decrease at the ortho II-I transition point at $\tau=0.96$. In sharp contrast, on the α_2 sublattice, there is almost zero occupancy by oxygen till the onset of the single-cell phase where distinction between α_1 and α_2 vanishes. Due to these radically opposite behaviors, the average site occupancy (marked α_{av}) develops a distinct plateau in the cell-doubled region.

The pair probabilities $x_2^{\alpha_1}$, $x_2^{\alpha_2}$ behave similarly to the associated point probabilities described above. This behavior suggests that under conditions of constant p_{O_2}, the formation of O-Cu-O chains remains fairly constant in the entire cell-doubled region, as shown by the average pair probability curve in Fig. 8, whereas it increases rapidly in the single-cell region. In previous work, similar pair probabilities were examined, however under conditions of fixed temperature. The plateau effect was also observed in the cell-doubling regime.[10]

Both the concentration range and plateau structure suggest that the plateau in the superconducting critical temperature and dip in room-temperature resistivity seen by Cava *et al.*[18] is related to the presence of the ortho-II phase. As pointed out previously, equilibrium long-range order may be difficult to achieve for this phase due to kinetic reasons; however, at least a short-range order state could have been observed.[18]

VII. DISCUSSION

A basic assumption underlying the present study is that all oxygen gain and loss by the 1:2:3 compound can be taken into account by oxygen concentration changes in the basal plane. Accordingly, it was possible to relate the stoichiometry index z to the planar concentration c_0 by the equation $z=2(c_0+3)$, resulting in a one-to-one correspondence between the two oxygen scales shown at top and bottom of Fig. 3. The assumption in question is clearly an oversimplification: It is known that oxygen loss tends to create planar defects, particularly near the surface of samples examined in transmission electron microscopy (TEM).[39] Furthermore, recent neutron-diffraction evidence shows that as much as 10% vacant sites can occur on O(4) oxygen sites, i.e., those bridging chain and puckered plane Cu sites.[40]

The compound under study is very much an open thermodynamic system and its oxygen content cannot be measured or controlled accurately. As a result, much controversy exists concerning the oxygen concentrations at which the orthorhombic-to-tetragonal transition takes place. The present calculation (completed before the experimental results were available) agrees well with the data obtained by investigators at the Oak Ridge National Laboratory.[38] Other measurements[4,40] indicate that the transition, at equilibrium, occurs invariably at or very close to stoichiometry $z=6.5$, regardless of the oxygen partial pressure under which the experiment is carried out. Although 6.5 is exactly midway between the "pure" stoichiometries $z=6$ and $z=7$, there is no thermodynamic reason for the transition to be located exactly at this composition. Moreover, the second-order line shown in Figs. 2 and 3 must necessarily deviate from the vertical at high temperatures, or at high p_{O_2} so as to meet the vertical at $c_0=0.5$. It merely appears, over the narrow range of transition temperatures and oxygen partial pressures conveniently available to experiment, that the transition line is practically vertical in the phase diagram. The CVM calculations do not show such behavior, but it is known that Monte Carlo results for $V_2=V_3$, tend to exhibit this property over a certain temperature range. Such calculations are now in progress.

Many measurements have been performed on samples prepared in a nonequilibrium manner by quenching from a high temperature.[18] In particular, Jorgensen *et al.*[40] report that quenched samples appear to transform from the tetragonal to ortho-I phases at lower starting stoichiometries than do equilibrium ones. These authors speculate that the material actually picks up oxygen during the quenching operation. The present authors prefer the alternative explanation given by Jorgensen *et al.*[40] which is that, at lower temperatures, the order-disorder transition line bends over towards the oxygen-poor concentrations, as calculated in the present work, and as seen in Figs. 2 and 3, for example.

Some controversy surrounds the existence of the ortho-II phase, as well. Initially, evidence for cell doubling was available only from (TEM) studies[16,17] which showed faint diffraction spots (or streaking) centered on $\langle \frac{1}{2}00 \rangle$ points in electron-diffraction patterns. Neutron diffraction revealed no such superlattice reflections until very recently.[41] Now, however, well-defined $\langle \frac{1}{2}00 \rangle$ maxima have been observed in x-ray-diffraction patterns of single crystals by Fleming *et al.*[37] Moreover, Meissner effect studies[18,40] have clearly shown the existence of a plateau in the value of the superconducting T_c (at about 60 K) in the vicinity of the ortho-II oxygen composition suggesting the existence of a well-defined and separate ordered phase. Its experimental detection is certainly hampered by the fact that, according to our phase-diagram calculations (Fig. 3 and also Fig. 2 of Ref. 10), ortho II is stable only below about 400 °C, i.e., in temperature ranges where oxygen mobility is extremely low, precluding complete ordering.

Very recently, new experimental evidence has confirmed the validity of the ortho-I–ortho-II equilibrium phase diagrams models: Chen *et al.*[42] have performed dark-field TEM with aperture centered on the $\langle \frac{1}{2}00 \rangle$ superlattice spots revealing small domains with double-cell structure in a background of the single-cell orthorhombic phase. It can only be concluded that low-temperature equilibrium is a two-phase mixture of ortho I and ortho II, which is in full agreement with the predictions derived from the phase diagram of Fig. 3 or that of our previous publication.[10] Low-temperature two-phase coexistence

between tetragonal ($z \cong 6$) and ortho-I ($z \cong 7$) phases is thereby excluded, indicating that the model leading to the phase diagram of Fig. 3 is preferred over that leading to Fig. 2. Consequently, the parameter V_3 must be positive, i.e., leading to chain ordering along the a axis. Furthermore, by establishing a correspondence between oxygen content and lattice parameter, You *et al.*[43] were able to measure, by x-ray diffraction, tie-line extremities which agreed closely with those shown in our previous ortho-I/ortho-II phase diagram.[10]

Diffuse diffraction spots have been reported at other locations in electron-diffraction patterns but evidence for additional ordered structures is by no means unambiguous. Ground-state analysis disallows ordering beyond that described in Ref. 7 for interactions extending only to second neighbors. If more distant pair interactions of sufficient magnitude existed along the a direction, other, more complicated parallel chain ordering could result. Conditions under which such ordering could take place were studied in detail by Finel[26] for the one-dimensional Ising model with pair and multisite interactions out to fifth neighbor. If it were to prove necessary, CVM phase diagrams could be calculated with more long-range interactions, resulting in additional low-temperature ordered-phase regions, but the calculations would be quite cumbersome.

It has been suggested recently[44] that chain ordering is only fortuitously related to superconductivity in $YBa_2Cu_3O_x$. The present authors are not attempting to relate directly the oxygen ordering to the superconducting transition. Rather, the thermodynamics of the 1:2:3 compound is investigated for its own sake and for its potential usefulness in processing of this material.

VIII. CONCLUSION

A two-dimensional Ising model with one first and two second-neighbor effective pair interactions is used to study the structural behavior of the Cu-O basal plane of the 1:2:3 compound. Two new phase diagrams for the oxygen-vacancy system have been calculated. Both diagrams have the experimentally observed tetragonal-to-orthorhombic second-order transitions with stable ortho-I phase near $x=7$. In one case, the "tricritical model," ortho I and tetra are the only two phases which are found to be stable. The two-phase regions are separated by a second-order transition line from above a tricritical point and a miscibility gap from below. The other diagram, the "cell-doubling model," has in addition to the above two phases a cell-doubled phase, near $x=6.5$, denoted ortho II.

For the latter diagram it was found that, by fitting the magnitude of V_1, experimentally determined transition points fell very nearly on the second-order line. Based on this fit, constant oxygen partial pressure isobars were calculated. Calculated oxygen point (site occupancy) and pair probabilities agreed reasonably well with experiment at $p_{O_2}=1$ atm.

Experimental confirmation of a cell-doubled phase is now well established. However, phase separation at low temperature, which is also predicted by the present diagrams, still awaits unambiguous confirmation: oxygen kinetics at these low temperatures are very sluggish, making experimental phase equilibrium determination very difficult.

ACKNOWLEDGMENTS

The authors benefited greatly from interesting conversations with many colleagues; among these are B. Batlogg, J. Jorgensen, S. C. Moss, C. J. Sparks, and L. T. Wille. Consultations with Staff Scientist, Martin Gelbaum, about Lawrence Berkeley Laboratory computing services are greatly appreciated. One of us (A.B.) was partially supported by a grant from the National Science Foundation. This work was supported by a grant from the Director, Office of Energy Research, Materials Sciences Division, U.S. Department of Energy, under Contract No. DE-AC03-76SF00098.

[1] J. G. Bednorz and K. A. Müller, Z. Phys. B **64**, 189 (1986).
[2] M. K. Wu, J. R. Ashburn, C. J. Torny, P. H. Hor, R. L. Meng, L. Gao, Z. J. Huang, Y. Q. Wang, and C. W. Chu, Phys. Rev. Lett. **58**, 908 (1987).
[3] H. Maeda, Y. Tanaka, M. Fukutomi and T. Asano, Jpn. J. Appl. Phys. Lett. (to be published).
[4] Y. Guo, J.-M. Langlois, and W. A. Goddard III, Science **239**, 896 (1988).
[5] J. D. Jorgensen *et al.*, Phys. Rev. B **36**, 3608 (1987).
[6] D. de Fontaine, L. T. Wille, and S. C. Moss, Phys. Rev. B **36**, 5709 (1987).
[7] L. T. Wille and D. de Fontaine, Phys. Rev. B **37**, 2227 (1988).
[8] A. Berera, L. T. Wille, and D. de Fontaine, J. Stat. Phys. **50**, 1245 (1988).
[9] L. T. Wille, A. Berera, D. de Fontaine, and S. C. Moss, Mater. Res. Soc. Symp. Proc. **99**, 535 (1988).
[10] L. T. Wille, A. Berera, and D. de Fontaine, Phys. Rev. Lett. **60**, 1065 (1988).
[11] A. Berera, L. T. Wille and D. de Fontaine, in *Proceedings of the International Conference on High-Temperature Superconductors: Materials and Mechanisms of Superconductivity, Interlaken, Switzerland, 1988* edited by J. Müller and J. L. Olsen [Physica C **153–155**, 598 (1988)].
[12] D. de Fontaine, in *Electronic Band Structure and its Application,* edited by M. Yussouff (Springer-Verlag, Berlin, 1987), pp. 410–430.
[13] A. Berera, H. Dreyssé, L. T. Wille, and D. de Fontaine, J. Phys. F **18**, L49 (1988).
[14] F. Ducastelle and F. Gautier, J. Phys. F **6**, 2039 (1976).
[15] F. Ducastelle, J. Phys. C **8**, 3297 (1975).
[16] M. A. Alario-Franco, J. J. Capponi, C. Chaillout, J. Chenevas, and M. Marezio, Mater. Res. Soc. Symp. Proc. **99**, 1685 (1988).
[17] G. Van Tendeloo, H. W. Zandbergen, and S. Amelinckx, Solid State Commun. **63**, 603 (1987).
[18] R. J. Cava, B. Batlogg, C. H. Chen, E. A. Rietman, S. M. Zaburak, and D. Werder, Phys. Rev. B **36**, 5719 (1987).
[19] K. Binder and D. P. Landau, Phys. Rev. B **21**, 1941 (1980).

[20]F. Claro and V. Kumar, Surf. Sci. **119**, L371 (1982).
[21]P. A. Rikvold, W. Kinzel, J. D. Gunton, and K. Kaski, Phys. Rev. B **28**, 2686 (1983).
[22]R. Kikuchi, Phys. Rev. **81**, 988 (1951).
[23]D. M. van Baal, Physica **64**, 571 (1973).
[24]D de Fontaine, in Proceedings of the NATO Institute on Phase Stability, Crete, 1987 (unpublished).
[25]J. M. Sanchez, F. Ducastelle, and D. Gratias, Physica A **128**, 334 (1984).
[26]A. Finel, These de Doctorat, Université Pierre et Marie Curie, France, 1987, edited by A. Gonis and G. M. Stocks (unpublished).
[27]J. Kulik and R. Kikuchi (private communication).
[28]J. M. Sanchez and D. de Fontaine, Phys. Rev. B **21**, 216 (1980).
[29]J. M. Bell, Phys. Rev. B **37**, 541 (1988).
[30]H. Bakker, D. O. Welch, and O. W. Lazareth, Solid State Commun. **64**, 237 (1987).
[31]A. G. Khachaturyan, S. V. Semenovskaya, and J. W. Morris, Jr., Phys. Rev. B **37**, 2243 (1988).
[32]A. G. Khachaturyan and J. W. Morris, Jr., Phys. Rev. Lett. **59**, 2776 (1987).
[33]Z.-X. Cai and S. D. Mahanti, Phys. Rev. B **36**, 6928 (1987).
[34]A. Finel and D. de Fontaine, J. Stat. Phys. **43**, 645 (1987).
[35]S. M. Allen and J. W. Cahn, in *Alloy Phase Diagrams,* edited by L. M. Bennett, T. B. Massalski, and B. C. Giessen, Materials Research Society Proceedings, Vol. 19 (Materials Research Society Pittsburgh, 1983), p. 195.
[36]D. de Fontaine, Acta Metall. **23**, 533 (1975).
[37]R. M. Fleming, L. F. Schneemeyer, P. K. Gallagher, B. Batlogg, L. W. Rupp, and J. V. Waszczak, Phys. Rev. B **37**, 7920 (1988).
[38]E. D. Specht, C. J. Sparks, A. G. Dhere, J. Brynestad, O. B. Cavin, D. M. Kroeger, and H. A. Oye, Phys. Rev. B **37**, 7426 (1988).
[39]H. W. Zandbergen, R. Gronsky, K. Wang, and G. Thomas, Mater. Res. Soc. Symp. Proc. (to be published).
[40]J. D. Jorgensen, H. Shaked, D. G. Hinks, B. Dabrowski, B. W. Veal, A. P. Paulikas, L. J., Nowicki, G. W. Crabtree, W. K. Kwok, L. H. Nunez, and H. Claus, in *Proceedings of the International Conference on High-Temperature Superconductors: Materials and Mechanisms of Superconductivity, Interlaken, Switzerland, 1988,* edited by J. Müller and J. L. Olsen [Physica C **153–155**, 578 (1988)].
[41]S. K. Sinha (private communication).
[42]C. H. Chen, D. J. Werder, L. F. Schneemeyer, P. K. Gallagher, and J. V. Waszczak, Phys. Rev. B **38**, 2888 (1988).
[43]H. You, J. D. Axe, X. B. Kan, S. Hashimoto, S. C. Moss, J. Z. Liu, G. W. Crabtree, and D. J. Lam (unpublished).
[44]Y. Tokura, J. B. Torrance, T. C. Huang, and A. I. Nazzal (unpublished).